

# Electrical and Optical Characterization of Gliding Arc Discharge (GAD) Operated at Line Frequency (50 Hz) Power Supply

*S. Dhungana, R. Prakash Guragain, H. B. Baniya,  
G. P. Panta, G. Kunwar Chhetri, D. P. Subedi*

**Journal of Nepal Physical Society**

*Volume 6, Issue 2, December 2020*

*ISSN: 2392-473X (Print), 2738-9537 (Online)*

**Editors:**

Dr. Binod Adhikari

Dr. Bhawani Joshi

Dr. Manoj Kumar Yadav

Dr. Krishna Rai

Dr. Rajendra Prasad Adhikari

Mr. Kiran Pudasainee

*JNPS, 6 (2), 26-33 (2020)*

DOI: <http://doi.org/10.3126/jnphysoc.v6i2.34852>

**Published by:**

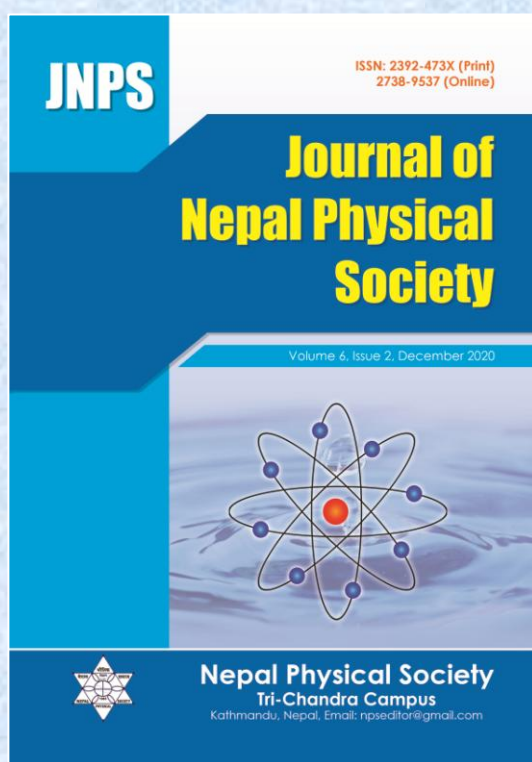
**Nepal Physical Society**

P.O. Box: 2934

Tri-Chandra Campus

Kathmandu, Nepal

Email: [npseditor@gmail.com](mailto:npseditor@gmail.com)





## Electrical and Optical Characterization of Gliding Arc Discharge (GAD) Operated at Line Frequency (50 Hz) Power Supply

S. Dhungana<sup>1,\*</sup>, R. P. Guragain<sup>1</sup>, H. B. Baniya<sup>1,2</sup>, G. P. Panta<sup>1</sup>, G. K. Chhetri<sup>1</sup> and D. P. Subedi<sup>1</sup>

<sup>1</sup>Department of Physics, School of Science, Kathmandu University, Dhulikhel, Nepal

<sup>2</sup>Department of Physics, Tri-Chandra Multiple Campus, Tribhuvan University, Kathmandu, Nepal

\*Corresponding Email: [sanein1@yahoo.com](mailto:sanein1@yahoo.com)

---

*Received: 16 October, 2020; Revised: 16 November, 2020; Accepted: 23 December, 2020*

---

### Abstract

In this study, an atmospheric alternating-current gliding arc device using line frequency (50 Hz) has been designed for the generation of various reactive species in different working gases. Electrical characteristics of the generated discharge are investigated by oscilloscope while the optical characteristics are analyzed using optical emission spectroscopy. The role of different working gases (oxygen, argon and air) on discharge voltages and power consumption per cycle in the discharge are calculated and compared. Electron density and electron temperature of the discharge are estimated by electrical and optical method respectively. The production of reactive species in the discharge is affirmed by optical emission spectroscopy. The outcomes of the results confirm that the GAD can generate non-equilibrium plasma having reactive nitrogen and oxygen species (RONS) which are essential for plasma chemistry applications.

**Keywords:** Non-thermal plasma, Reactive species, Discharge voltage, Electron density, Electron temperature.

### 1. INTRODUCTION

Among several discharge system to generate plasma, gliding arc discharge (GAD) is the emerging technique to produce non-thermal plasma. It is considered to be a transitional discharge and can be generated by applying an electrical field across a pair of diverging electrodes [1]. It involves higher quantities of energy than other cold discharges at atmospheric pressure. The discharge or arc is produced in the shortest gap between the two or three divergent electrodes. Then arc is forced to move downward by a stream of gas and is convectively cooled by a stream of room-temperature gas, becoming a non-equilibrium discharge [2]. The plasma generated by the gliding arc discharge has thermal or non-thermal properties depending on the system parameters such as power input and flow rate [3]. Non-thermal type of plasma which has electron temperature much greater than gas temperature is a source of high energy electrons and essential for typical plasma chemistry applications [4].

In recent years, the applications of gliding arc discharge are grooming in various fields because it is able to generate a large amount of active plasma species. Mainly, the GAD is used to remove organic dye from the polluted water by oxidizing the impurities [5, 6, 7]. Bo et al. (2008) reported that it can be used for decomposition of greenhouse gases into other synthesis gases [8]. Wang et al. (2017) used GAD to convert CO<sub>2</sub> to CO and O<sub>2</sub>, indicating that the non-equilibrium nature of the discharge allows for much higher energy efficiency compared to classic thermal method [9]. In biomedical field, it has been used for inactivation of microorganism as it is used to treat water to sterilize the bacteria [10]. Kim et al. (2013) mentioned in their report that plasma generated from GAD was able to perform a total 6-log reduction in the cfu (colony-forming unit) counts of Escherichia Coli within 25 min of duration [2]. Besides this, GAD can be used to generate plasma activated water (PAW) [11], in food sterilization [12, 13], in surface modification [14] and in agriculture [15, 16].

Plasma diagnostics is crucial for the understanding of the discharge physics which helps to estimate the most fundamental parameters (electron density and electron temperature) in gas discharges [17]. The plasma parameters are strongly dependent upon the type of discharge, nature of working gas, gas pressure, power supply geometrical structure of electrodes, materials of dielectrics etc. [18].

The primary goal of this research is to understand the nature and quality of the discharge using optical and electrical means. Using the electrical method, role of gas in breakdown voltages at atmospheric pressure is studied and consumption of powers in different gases are calculated. Also, electron densities on various working gases and voltages are determined and compared. From optical method, formation of highly reactive nitrogen and oxygen species are confirmed over the interface between air and water surfaces. One of the important characteristics of plasma i.e. electron temperature is also calculated from optical method by using Boltzmann's plot method where different lines of nitrogen and argon are used.

## 2. EXPERIMENTAL SET UP

The schematic diagram of the experimental setup is shown in Fig. 1. The system consists of two diverging electrodes made up of aluminium. The two electrodes are attached to a rectangular polycarbonate chamber with dimension ( $15\text{ cm} \times 15\text{ cm} \times 15\text{ cm}$ ). A small hole is made on the upper face of the chamber to inlet the gas. Three types of gas viz. air, oxygen and argon are passed through the gas inlet. The minimum gap between the electrodes is maintained at 3 mm. A beaker is placed underneath the electrodes for the treatment of water. High voltage transformer (0-18 kV, 50 Hz) is used as a power source for the generation of discharge. Ballast resistor of 1.7 M $\Omega$  is used to limit the high current and a shunt resistor of 10 k $\Omega$  is used to measure the current in the circuit. A current probe and a PINTEX high voltage probe (attenuation ratio 1000:1) are connected to digital oscilloscope (Tektronix TDS2000) along with a computer to capture the waveforms. In order to take the optical spectra by using optical fibre, a small hole is made at one face of the chamber. The optical emission spectra are measured by an optical fibre through the hole keeping the position of the fibre fixed to 4 cm far from discharge. The emission spectra of the produced GAD plasmas are registered with a computer associating a Digital Spectrometer (Ocean Optics: USB 2000+).

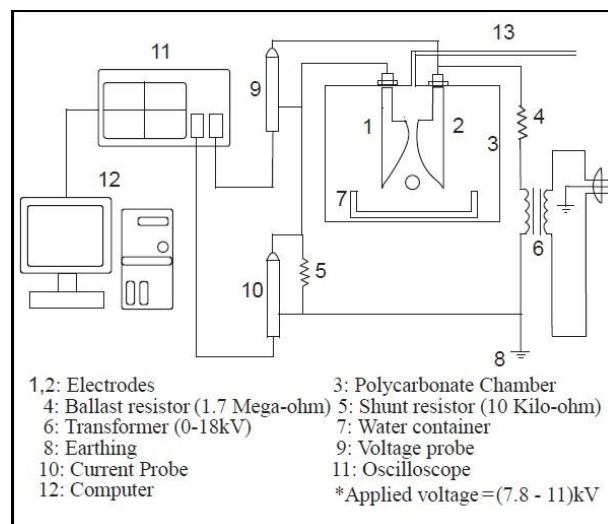


Fig. 1: Schematic diagram of experimental arrangement of GAD system

## 3. RESULTLS AND DISCUSSION

### 3.1. Electrical characterization

#### 3.1.1 IV Characteristics

When electric field is applied between the electrodes, it accelerates free electrons and transfers their momentum to the neutral gas molecules. Through several collision mechanisms the gas molecules are ionized which results in the arc ignition [19]. Fig. 2 shows the voltage-current waveforms of the GAD air plasma measured at an applied voltage of 9.3 kV and electrode spacing of 3 mm. The figure depict that the current waveform appears to be sinusoidal while the voltage waveform is quite different from the normal voltage waveform and resembles sawtooth shape. Here, in sawtooth type arc voltage waveform, two different arc breakdown regimes can be identified. They are: breakdown in the narrowest gas gap and breakdown on the electrode surface [20]. Initially, at the shortest electrode gap, the voltage reaches maximum value and the arc is created following the initial breakdown. This type of breakdown is characterized by peaks (A) as shown in figure 2(b). In this moment the resistance of the arc is almost zero and the current spikes dramatically. Then due to the leakage flux of the Transformer current provided by it is reduced. After few milliseconds the developed arc is pushed downward along the electrodes and length of plasma column increases. At this moment the voltage suddenly drops when the restrike breakdown, a re-establishment of the fast breakdown, occurs in cold gas layers on the electrode wall and the breakdown peaks (B) are

observed as shown in Fig. 2(b) [20]. The increase in column length of plasma cannot be sustained by the input energy of the power supply and finally the plasma extinguishes [21]. At this point the recombination starts and re-ignition of the

discharge occurs at the shortest gap of the electrodes. A third type of irregular peaks (C) can also be observed in the wave form. These are caused by the small scale restrike break down far from the shortest gap [20].

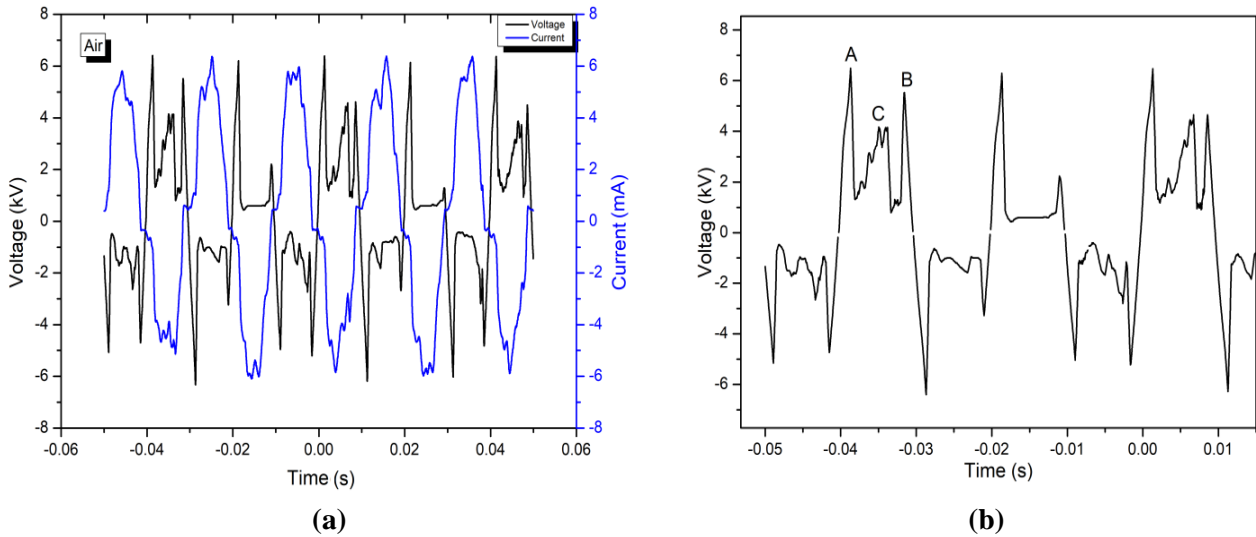


Fig. 2: Figure showing (a) current voltage waveform and (b) breakdown voltages in air at 9.3 kV.

In order to study the variation of breakdown voltage with gas, different gases (air, argon and oxygen) are passed through the nozzle and their respective voltages are recorded through the oscilloscope. The Fig. 3(b) clearly shows the role of gases in breakdown voltage or discharge voltage. The discharge voltage varies for different working gases because the ionization energy or electron

impact ionization cross section is different among the gases [22]. For argon the breakdown voltage is smaller than that of air and oxygen and, it breaks down faster than air and oxygen. The graph also shows that air requires more voltage than that of oxygen to start a discharge or electric arc between two electrodes which agree with the Paschen's law [23].

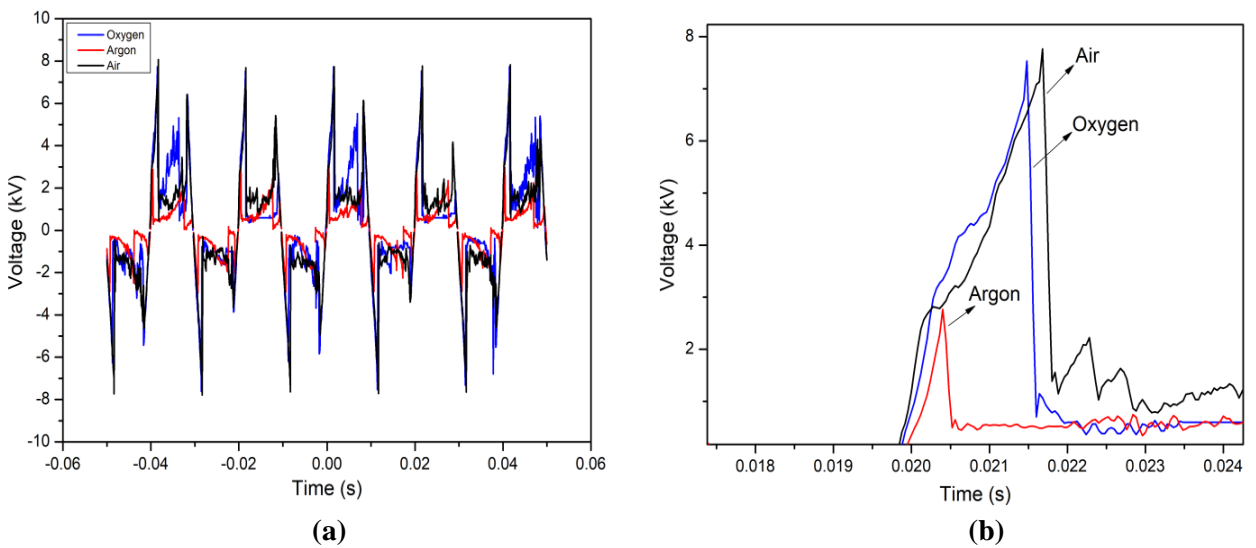


Fig. 3: (a) Variation of voltage wave form at different gases and (b) breakdown voltage for different gases

### 3.1.2 Power Consumption

Using the voltage and current waveforms of the GAD plasma, the consumed power (P) can be calculated by the following equation:

Where, T is the time period and  $i(t)$  and  $v(t)$  are the current and voltage of the GAD plasma [19].

$$P = \frac{1}{T} \int_0^T i(t)v(t)dt \dots \dots \dots (1)$$

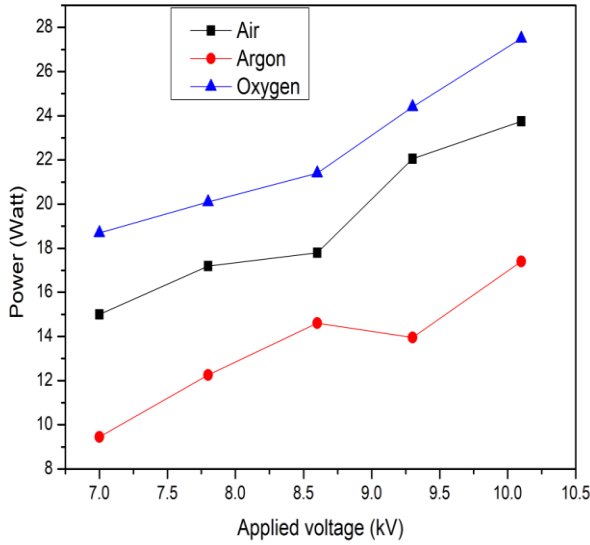


**Fig. 4:** Variation of consumed power by air, argon and oxygen plasma with different applied voltages

The work is devoted to the study of the effect of fading gases on the power consumption of gliding arc discharge. Fig. 4 shows the variation of consumed power by air, argon and oxygen plasma with applied voltages. It shows that as the applied voltage increases the power consumption by the discharge increases in all these working gases. Among all three working gases the discharge dissipated least power in argon and more in oxygen. Although the discharge current in all three types of gases are nearly equal, the breakdown voltage for different gases vary. Hence the powers dissipated in the discharge are not the same for all working gases. The discharge voltages vary during different working gases because the ionization energy or electron impact ionization cross sections also vary among the gases [22]. Peak current is high in argon environment in comparison to other two gases. However, its breakdown voltage is quite lower compared to the others, and therefore, it consumed least power.

### 3.1.3 Electron Density ( $n_e$ )

The electron density is an important factor to determine the properties of plasma species. From the electrical method the electron density is calculated following equation [24, 25]

$$n_e = \frac{j}{eE\mu_e} \dots \dots \dots (2)$$

Where,

$j = \frac{i}{A}$  = current density,  $i$ =discharge current,

$A$ =cross sectional area of plasma,

$e$  = electronic charge= $1.6 \times 10^{-19} C$

$E = \frac{V}{d}$  = Electric field,  $V$ = breakdown voltage,

$d$ =distance between the electrodes

$\mu_e$  = Electron mobility

In our case, cross sectional area of the plasma =  $0.48 \text{ cm}^2 - 0.60 \text{ cm}^2$ , discharge voltage = 2.8 kV to 7.5 kV, discharge current = 47 mA to 75 mA, minimum distance between the electrodes = 0.3 cm. The mobility of electron in argon and air is  $434 \text{ cm}^2\text{V}^{-1}\text{s}^{-1}$  and  $592.1 \text{ cm}^2\text{V}^{-1}\text{s}^{-1}$  respectively [26].

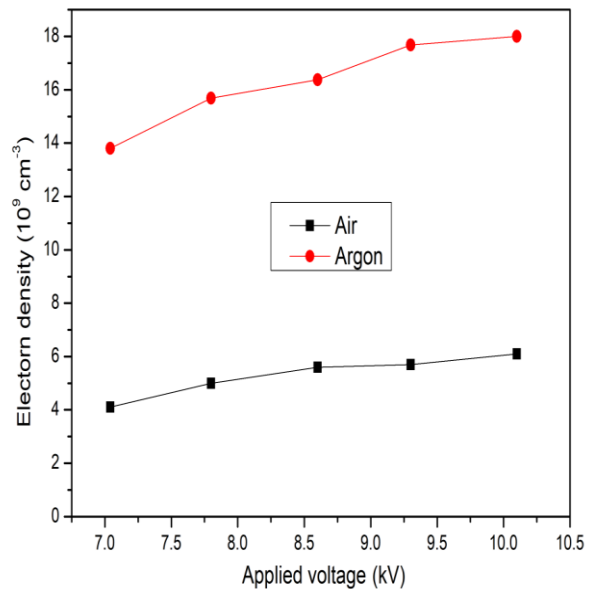


**Fig. 5:** Variation of electron density with applied voltage for air and argon discharge

Using equation (2) and the above parameters, the electron densities of the discharge were calculated for argon and air. Fig. 5 shows the

graphical representation of the variation of electron density with applied voltage for air and argon. It is observed from the Fig. 5 that electron density increases as the applied voltage increases for both the cases. This shows that as the more power dissipate in the discharge, more electron density is generated which agree with previous work by Xiao et al. (2014) [15]. If we compare the electron density of argon and air plasma, electron density in case of argon is about three times greater than that of air plasma. This is due to the fact that breakdown voltage of argon is less than that of air. As a result, large numbers of argon atoms ionize easily which produce pool of secondary electrons. But in case of air, the dissociative recombination between the electrons and nitrogen molecular ions as well as electron and oxygen molecular ions takes place [27].

**4. OPTICAL CHARACTERIZATION**

Optical emission spectroscopy (OES) is not only used to determine the plasma parameters like plasma temperature and electron density but also used to detect the reactive oxygen and nitrogen species produced by the discharge. It enables us to determine the rotational, vibrational and electronic excitation temperatures of the plasma and thus the level of non-equilibrium [28]. Fig. 6 shows the typical optical emission spectrum of air gliding arc discharge. By investigating through the optical emission spectroscopy (OES) valuable information on excited atomic and molecular states can be obtained. The emission profile from 200 to 400 nm is mostly composed of reactive nitrogen as well as oxygen species. In our case, presence of  $NO\gamma$  (200-280 nm), OH (309 nm),  $N_2$  second positive system (SPS) (311-380 nm),  $N_2$  first negative system (FNS) around 400 nm [29] in the spectrum suggests that the discharge can form reactive nitrogen and oxygen species (RNOS) above the water during the preparation of Plasma Activated Water (PAW). The formations of these species are due to the collision of energetic electrons with nitrogen and oxygen molecules present in the ambient air. OH radicals are emitted at 309 nm and considered to be originated from the collision of electrons, or metastable nitrogen atoms, with water molecules [28]. Similarly, the excited nitrogen species originate from the dissociation of nitrogen molecules present in ambient environment or feeding gas [30].

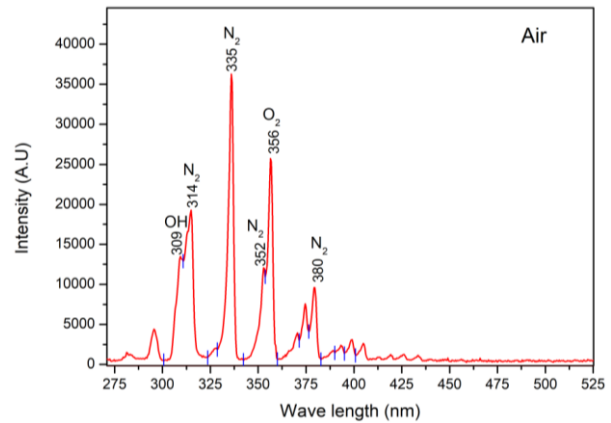


**Fig. 6:** Optical spectra of air plasma and reactive oxygen and nitrogen species.

**4.1 Calculation of Electron Temperature**

An important parameter representing plasma properties is electron temperature which directly reflects the average kinetic energy of the electrons in the plasma [31]. There are various methods that can be used to calculate the electron temperature such as double-line method, multispectral line slope method, the Saha–Boltzmann method, and absolute line intensity method etc. In our case, in order to calculate the electron temperature, Boltzmann plot method is used. Boltzmann plot method is a simple and widely used method for spectroscopic measurement, especially for measuring the electron temperature of plasma by using the relative intensity of two or more line spectra having a relatively large energy difference [32]. The electron temperatures are calculated for air and argon discharge by using equation (3) [33, 34].

$$\ln \left[ \frac{I_{ij} \lambda_{ji}}{A_{ji} g_j} \right] = - \frac{E_j}{k T_e} + C \dots\dots\dots(3)$$

Where,

- $I_{ij}$  = Intensity of emitted light
- $\lambda_{ji}$  = Wave length of emitted light
- $A_{ji}$  = Transition probability
- $g_j$  = Statistical weight of upper level
- $E_j$  = Upper energy level
- $k$  = Boltzmann constant
- $T_e$  = Electron temperature
- $C$  = Constant

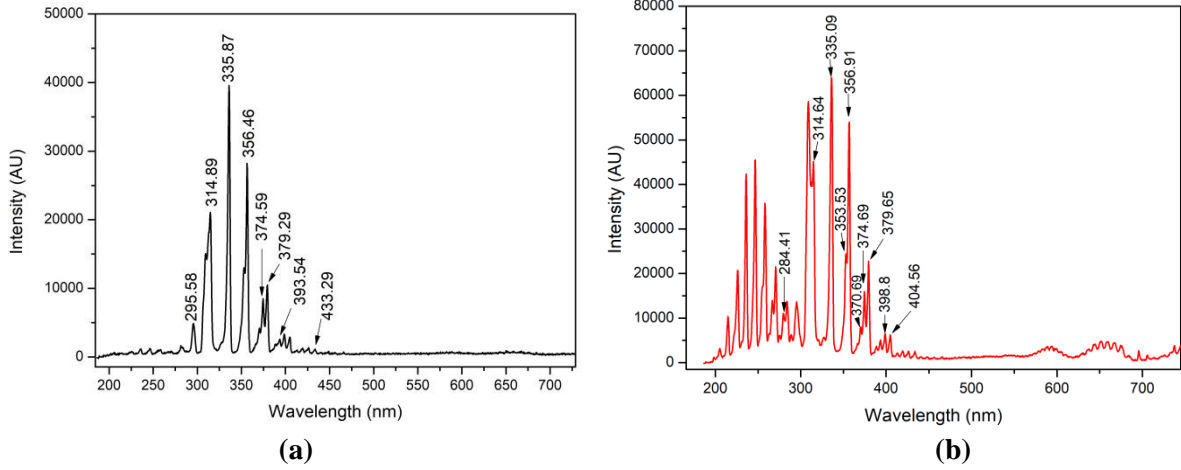


Fig. 7: Variation of intensities with wavelength of (a) air and (b) argon discharge

Figure 7a and 7b show the spectra of the discharge and their corresponding intensities, and wavelengths at an atmospheric pressure gliding arc discharge in air and argon respectively. In Boltzmann plot method nitrogen III (NIII) lines and argon II (Ar II) lines with their respective intensities and energies are chosen. The spectroscopic data required for the Boltzmann plot

are collected from NIST database [19]. Graphs are plotted with  $E_{ji}$  in horizontal axis

and  $\ln \left[ \frac{I_{ij} \lambda_{ji}}{A_{ji} g_j} \right]$  in the vertical axis which give fitted straight lines as shown in Fig. 8. Finally, electron temperature is estimated from the slope of the straight line.

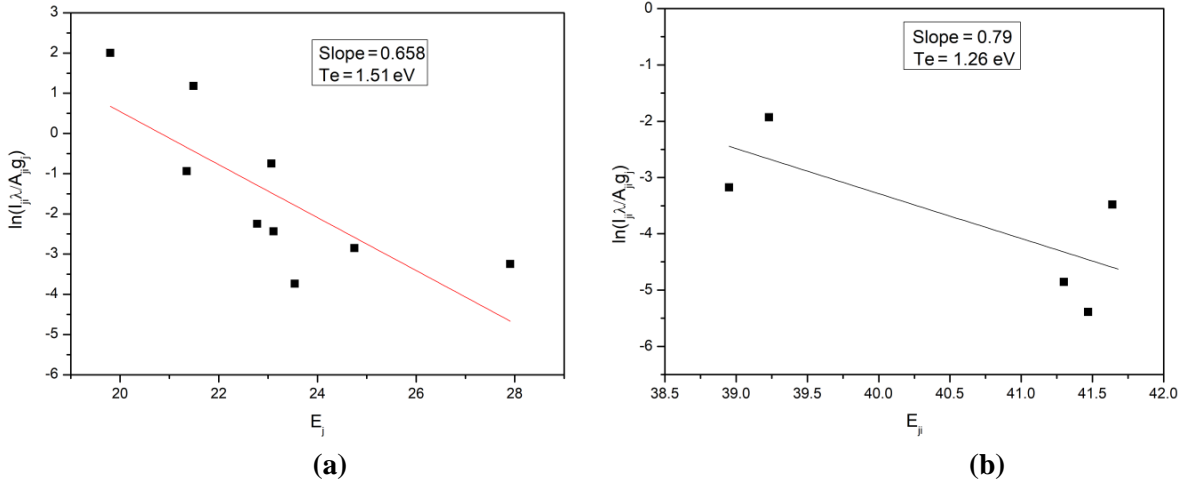


Fig. 8: Determination of slope and  $T_e$  of the discharge for working gas (a) argon and (b) air

From Fig. 8, electron temperature for the argon and air are found to be 1.51 eV and 1.26 eV respectively. The electron temperature of the discharge with argon as a working gas is higher than that of discharge in the air for same applied voltage. This is due to the fact that the breakdown voltage for argon gas is less than that of the air. As a result it contains more concentration of energetic electrons at lower voltage than that of air. These

electrons can excite the particles to transit between the high-energy states and generate more active particles with high energetic electrons [29] resulting more  $T_e$  in argon environment than in air.

## 5. CONCLUSIONS

In this work, custom made GAD system operating at line frequency (50 Hz) is used to produce

discharge and characterization of such discharge is done by electrical and optical method. From above result, it is confirmed that breakdown voltage on gliding arc discharge depends on the working gas. Breakdown voltage for argon is found to be less in comparison to oxygen and air. Due to more discharge voltage in oxygen and air, power consumptions in the discharge using these gases are found to be higher in comparison to argon. The electron density is estimated in the order of  $10^9 \text{ cm}^{-3}$  in both air and argon gas. The electron density increase slightly as the applied voltage increases. Formation of highly reactive nitrogen and oxygen species over the interface between air and water surfaces are confirmed by the optical spectra. The electron temperature in the discharge is calculated by using Boltzmann's plot method and is estimated to be 1.51 eV and 1.26 eV for argon and air plasma respectively. The value of electron density and electron temperature revealed that the gliding arc discharge can produce non-equilibrium plasma containing highly reactive species. Formation of these highly reactive species confirms the potential application of GAD on water treatment, food sterilisation and surface treatment.

#### ACKNOWLEDGEMENT

The corresponding author would like to acknowledge University Grants Commission (UGC) Nepal, for its financial support through award number MPhil-75/76-S&T-8. The authors would also like to acknowledge all the researchers of Kathmandu University Plasma Physics Laboratory and who provided valuable suggestion and help for the completion of the work.

#### REFERENCES:

- [1] Allah, Z. A. & Whitehead, J. C. Plasma-catalytic dry reforming of methane in an atmospheric pressure AC gliding arc discharge, *Catalysis Today* **30**: 1-4 (2015).
- [2] Kim, H. S.; Cho, Y. I.; Hwang, I. H.; Lee, D. H.; Cho, D. J.; Rabinovich, A. & Fridman, A. Use of plasma gliding arc discharges on the inactivation of *E. Coli* in water, *Separation and Purification Technology*, **120**: 423–428 (2013).
- [3] Yardimci, O. M.; Saveliev, A. V.; Fridman, A. A. & Kennedy, L. A. Thermal and non-thermal regimes of gliding arc discharge in air flow, *Journal of Physics*, **87**: 1632-1641 (2000).
- [4] Diatczyk, J.; Komarzyniec, G. & Stryczewska, H. D. Power Consumption of Gliding Arc Discharge Plasma Reactor, *International Journal of Plasma Environmental Science and Technology*, **5**: 12-16 (2011).
- [5] Burlica, R.; Kirkpatrick, M. J.; Finney, W. C.; Clark, R. J. & Locke, B. R. Organic dye removal from aqueous solution by glidarc discharges, *Journal of Electrostatics* **62**: 309–321 (2004).
- [6] Doubla, A.; Bello, L. B.; Fotso, M. & Brisset, J. L. Plasma chemical decolourisation of Bromothymol Blue by gliding electric discharge at atmospheric pressure, *Dyes and Pigments*, **77**: 118-124 (2008).
- [7] Njoyim, E. T.; Djokoa, Y. T.; Ghogomua, J.; Djepang, S. A. & Laminsi, S. Plasma-chemical treatment of industrial wastewaters from brewery “Brasseries du Cameroun”, Bafoussam factory, *Int. Journal of Engineering Research and Applications*, **6**: 60-71 (2016).
- [8] Bo, Z.; Yan, J.; Li X.; Chi, Y. & Cen, K. Plasma assisted dry methane reforming using gliding arc gas discharge: Effect of feed gases proportion, *International Journal of Hydrogen Energy*, **33**: 5545-5553 (2008).
- [9] Wang, W.; Mei, D.; Tu, X. & Bogaerts, A. Gliding arc plasma for CO<sub>2</sub> conversion: better insights by a combined experimental and modeling approach, *Chemical Engineering Journal*, **330**: 11–25 (2017).
- [10] Du, C. M.; Wang, J.; Zhang, L.; Li, H. X.; Liu, H. & Xiong, Y. The application of a non-thermal plasma generated by gas–liquid gliding arc discharge in sterilization, *New Journal of Physics*, **14**: 1-16 (2012).
- [11] Gharagozalian, M.; Dorrnian, D. & Ghoranneviss, M. Water treatment by the AC gliding arc air plasma, *Journal of Theoretical and Applied Physics*, **11**: 171–180 (2017).
- [12] Dasan, B. G.; Ulusoy, B. O.; Pawlat, J.; Diatczyk, J.; Sen, Y. & Mutlu, M. A. New and Simple Approach for Decontamination of Food Contact Surfaces with Gliding Arc Discharge Atmospheric Non-Thermal Plasma, *Food Bioprocess Technology*, **10**: 650–661 (2017).
- [13] Shaer, M. E.; Mobasher, M. & Abdelghany, A. Treatment of Microorganisms in Vegetables and Fruits by Gliding Arc, *Plasma Medicine*, **4**: 57-65 (2014).
- [14] Stranak, B. V.; Sery, M.; Tichy & Spatenka, M. P. Germination of *Chenopodium Album* in Response to Microwave Plasma Treatment, *Plasma Science and Technology*, **10**: 507-511 (2008).
- [15] Xiao, D.; Cheng, C.; Shen, J.; Lan, Y.; Xie, H. Shu, X.; Meng, Y.; Li, J. & Chu, P. K. Electron density measurements of atmospheric-pressure non-thermal N<sub>2</sub> plasma jet by Stark broadening and irradiance intensity methods, *Physics of Plasma*, **21**: 1-7 (2014).

- [16] Kogelschatz, U. Dielectric-barrier Discharges: Their History, Discharge Physics, and Industrial Applications, *Plasma Chemistry and Plasma Processing*, **23**: 1-46 (2003).
- [17] Faubert, F.; Wartel, M.; Pellerin, N.; Pellerin, S.; Cochet, V.; Regnier, E. & Hnatiuc, B. Treatment by gliding arc of epoxy resin: preliminary analysis of surface modifications, *Advanced Topics in Optoelectronics, Microelectronics, and Nanotechnologies*, **10010**: 1-11 (2016).
- [18] Pawlat, J.; Starek, A.; Sujak, A.; Kwiatkowski, M.; Terebun, P. & Budzeń M. Effects of atmospheric pressure plasma generated in glidar reactor on *Lavatera thuringiaca* L. seeds' germination, *Plasma Process and Polymers*, 1-11 (2017).
- [19] Roy, N. C. & Talukder, M. R. Effect of pressure on the properties and species production in gliding arc Ar, O<sub>2</sub>, and air discharge plasmas, *Physics of Plasma*, **25**: 1-8 (2018).
- [20] Tu, X.; Yu, L.; Yan, J. H.; Cen, K. F. and Chéron, B. G. Dynamic and spectroscopic characteristics of atmospheric gliding arc in gas-liquid two-phase flow, *Physics of Plasmas*, **16**: 1-5 (2009).
- [21] El-Zein, A.; Talaat, M.; El-Aragi, G. & El-Amawy, A. Electrical Characteristics of Nonthermal Gliding Arc Discharge Reactor in argon and nitrogen Gases, *Transactions on Plasma Science*, **44**: 1155-1159 (2016).
- [22] Attri, P.; Tochikubo F.; Park, J. H.; Choi, E. H.; Koga, K. & Shiratani, M. Impact of Gamma rays and DBD plasma treatments on wastewater treatment, *Scientific Report*, **8**(2926): 1-11 (2018).
- [23] Konuma, M. Film Deposition by Plasma Techniques, *Springer-Verlag, Heidelberg, Fed. Rep. of Germany* (1992).
- [24] Guragain, R. P.; Baniya, H. B.; Dhungana, S.; Gautam, S.; Pandey, B. P.; Joshi, U. M. & Subedi, D. P. Characterization Of Dielectric Barrier Discharge (DBD) Produced In Air At Atmospheric Pressure And Its Application In Surface Modification of High-Density Polyethylene (HDPE), *Journal of Technological and Space Plasmas*, **1**: 27-35 (2020).
- [25] Baniya, H. B.; Shrestha, R.; Guragain, R. P.; Kshetri, M. B.; Pandey, B. P. Subedi, D. P. Generation and characterization of an atmospheric pressure plasma jet (APPJ) and its application in the surface modification of polyethylene terephthalate. *International Journal of Polymer Science*, **2020**: 1-7 (2020).
- [26] Raizer, Y. P. *Gas Discharge Physics*, New York, NY, USA: *Springer* (1991).
- [27] Wang, Y.; Shi, J.; Li, C.; Feng, C. & Ding, H. Effect of Nitrogen Addition on Electron Density and Temperature of Cascaded Arc Argon Discharge Plasma Diagnosed by Laser Thomson Scattering, *IEEE Transactions on Plasma Science*, **47**: 1909-1916 (2019).
- [28] Ghimire, B.; Sornsakdanuphap, J.; Hong, Y. J.; Uhm, H. S.; Weltmann, K. D. & Choi, E. H. The effect of the gap distance between an atmospheric-pressure plasma jet nozzle and liquid surface on OH and N<sub>2</sub> species concentrations, *Physics of Plasmas*, **24**: 1-12 (2017).
- [29] Lamichhane, P.; Adhikari, B. C.; Nguyen, L. N.; Paneru, R.; Ghimire, B.; Mumtaz, S.; Lim, J. S.; Hong, Y. J. & Choi, E. H. Sustainable Nitrogen fixation from synergistic effect of photo-electrochemical water splitting and atmospheric pressure N<sub>2</sub> plasma, *Plasma Sources Science and Technology*, **29**: 1-10 (2020).
- [30] Adhikari, B.; Adhikari, M.; Ghimire, B.; Park, G. & Choi, E. H. Cold Atmospheric Plasma-Activated Water Irrigation Induces Defense Hormone and Gene expression in Tomato seedlings, *Scientific Reports*, **9** (16080), 1-15 (2019).
- [31] Chen, G. C.; He, L. M.; Zhao, B. B.; Zhang, H. L.; Zhao, Z. C.; Zeng, H.; Lei, J. P. & Liu, X. Effects of Working Medium Gases on Emission Spectral and Temperature Characteristics of a Plasma Igniter, *Journal of Spectroscopy*, **20**: 1-11 (2019).
- [32] Liu, G.; Yuan, P.; An, Sun, T. D.; Cen, J. & Wang, X. Using Saha-Boltzmann plot to diagnose lightning return stroke channel temperature, *Journal of Geophysical Research*, **124**: 4689-4698 (2019).
- [33] Ohno, N.; Razzak, M. A.; Ukai, H.; Takamura, S. & Uesugi, Y. Validity of Electron Temperature Measurement by Using Boltzmann Plot Method in Radio Frequency Inductive Discharge in the Atmospheric Pressure Range, *Plasma and Fusion Research*: **1 028**: 1-9 (2006).
- [34] Baniya, H. B.; Guragain, R. P.; Baniya, B. Subedi, D. P. Experimental study of cold atmospheric pressure plasma jet and its application in the surface modification of polypropylene, *Reviews of Adhesion and Adhesives*, **8** (2): 1-14 (2020).